ACS OMEGA

Article

Cite This: ACS Omega 2019, 4, 11135−11140

http://pubs.acs.org/journal/acsodf

Photocatalytic Hydrogen Production by RGO/$ZnIn_2S_4$ under Visible Light with Simultaneous Organic Amine Degradation

Ruijie Yang,[†,‡] Kelin Song,[†,‡] Jiansheng He,[†,‡,§] Yingying Fan,[†,‡] and Rongshu Zhu*[,†,‡]

[†]Shenzhen Key Laboratory of Organic Pollution Prevention and Control, Environmental Science and Engineering Research Center, and [‡]International Joint Research Center for Persistent Toxic Substances, Harbin Institute of Technology (Shenzhen), Shenzhen 518055, P. R. China

[§]Shanxi Acdemy of Analytical Sciences, Taiyuan 030006, P. R. China

ABSTRACT: In this work, the study of photocatalytic hydrogen production by RGO/$ZnIn_2S_4$ with simultaneous degradation of organic amines was carried out in the presence of organic amines in wastewater as the sacrificial agents. The effects of several factors, such as organic amine types, pH value, catalyst concentration, organic amine concentration, and sunlight source, on the photocatalytic activity of RGO/$ZnIn_2S_4$ for H_2 production were investigated. At the same time, its performance of degrading organic amines during H_2 production was also examined. The results showed that the order of H_2 production activity of RGO/$ZnIn_2S_4$ in six organic amine solutions was $N(CH_2CH_3)_3$ > $N(HOCH_2CH_2)_3$ > $N(CH_3)_3$ > $HO(CH_2)_2NH_2$ > $C_6H_5{-}N_2$ > $CO(NH_2)_2$, and the highest H_2 production was in $N(CH_2CH_3)_3$ (triethylamine) solution, being 1597 $\mu mol \cdot g^{-1} \cdot h^{-1}$, which is 2.6 times as high as that using the aqueous solution mixture of Na_2S and Na_2SO_3 as the sacrificial agent. In addition, when the pH was 13, the catalyst concentration was 1.0 $g \cdot L^{-1}$, and the triethylamine concentration was 1.0 $mol \cdot L^{-1}$, the photocatalytic activity was the highest. Furthermore, the relationship between triethylamine concentration and H_2 production was analyzed according to the theory of dynamics.

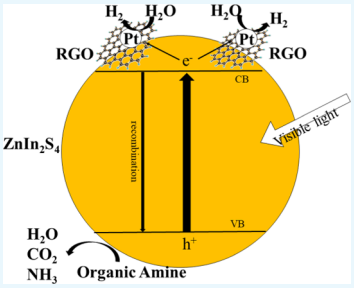

1. INTRODUCTION

With the development of social economy, the problems of environmental pollution and energy shortage have become increasingly pressing.[1−3] As a promising technology to generate new energy and solve environmental pollution, photocatalytic water-splitting for H_2 production has received extensive attention.[4−15] Currently, organic matters are usually used as sacrificial agents in the photocatalytic H_2 evolution technology because it can significantly enhance the H_2 production efficiency.[16−20] Furthermore, using organic pollutants in wastewater as the sacrificial agent can serve two purposes at the same time: increasing H_2 production and simultaneously removing the pollutant via oxidative decomposition.

Organic amines are common pollutants in the pharmaceutical, textile, and dyeing industries wastewater. The organic-amine-contaminated wastewater is high-nitrogen, poisonous, and difficult to biodegrade, thus threatening to the environment and human health. However, it is worth noting that the organic amines can be used as the effective sacrificial agents for photocatalytic H_2 production. In 2004, Wu et al.[21] studied the mechanism of oxygen-free photocatalytic H_2 production by TiO_2 in ethanolamine solution; the results showed that ethanolamine used as electron donor could improve H_2 production by TiO_2. In 2007, Yin et al.[22] studied photocatalytic H_2 production by TiO_2 in three different ethanolamine solutions; it was found that H_2 production with these three types of ethanolamine as the electron donors was much higher than that without electron donors, and the order of H_2 production in these solutions was triethanolamine > diethanolamine > monoethanolamine. In 2012, Li et al.[23] used $ZnIn_2S_4$ as the catalyst for photocatalytic H_2 production in triethylamine solution; it was found that using triethylamine as an electron donor significantly increased the H_2 production rate. In 2014, Peng et al.[24] studied photocatalytic H_2 production by $ZnIn_2S_4$ in the presence of three kinds of methylamine solutions; the results showed that the H_2 production activity of the catalyst was improved by using three types of methylamine as the electron donors; the activities of $ZnIn_2S_4$ in the three solutions was trimethylamine > dimethylamine > monomethylamine. The current reports mainly focus on the study of using organic amines as sacrificial agents to enhance photocatalytic H_2 production. Using organic amines in the wastewater as sacrificial agents to promote photocatalytic hydrogen evolution not only can achieve efficient conversion of pollutants and recovery of resource in water, but also can effectively prevent the organic-amine-contaminated wastewater to pollute the environment. However, the hydrogen production and simultaneous degradation of organic amines is rarely reported. Therefore, it is of great significance to study the simultaneous H_2 production and organic amine degradation with organic amines as sacrificial agents.

The previous study[25] of our research group showed that RGO/$ZnIn_2S_4$ has excellent photocatalytic H_2 production

Received: April 11, 2019
Accepted: June 14, 2019
Published: June 25, 2019

DOI: 10.1021/acsomega.9b01034
ACS Omega 2019, 4, 11135−11140

activity and stability under visible light. Based on the previous research on RGO/$ZnIn_2S_4$, in this work, the effects of several factors, such as organic amine species, pH value, catalyst concentration, organic amine concentration, and solar light source, on the photocatalytic hydrogen production activity of RGO/$ZnIn_2S_4$ were investigated, and then investigation was carried out about the degradation of organic amines in wastewater in the process of photocatalytic H_2 production. Furthermore, the relationship between triethylamine concentration and H_2 production was analyzed according to the theory of dynamics.

2. RESULTS AND DISCUSSION

2.1. Effects of Organic Amine Types on Photocatalytic H_2 Production. Figure 1 shows the photocatalytic

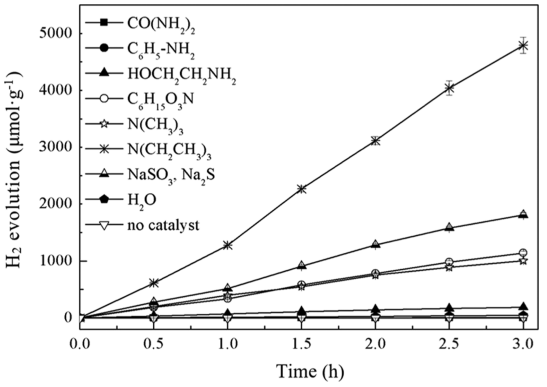

Figure 1. Photocatalytic H_2 production in different types of organic amine solutions.

H_2 production efficiency with different types of organic amines (urea, aniline, ethanolamine, triethanolamine, trimethylamine, and triethylamine) as sacrificial agents. For comparison, the H_2 production efficiency on the conditions of using Na_2S–Na_2SO_3 as the sacrificial agent, without the sacrificial agent (pure water), and using triethylamine without catalyst were also performed and are shown in Figure 1.

As can be seen from Figure 1, in the absence of RGO/$ZnIn_2S_4$, the H_2 production rate in the presence of 1.0 mol·L^{-1} triethylamine was 16 μmol·g^{-1}·h^{-1}, which could be ignored in comparison with that obtained using RGO/$ZnIn_2S_4$. In the solution containing only water molecules, the H_2 production rate by RGO/$ZnIn_2S_4$ was almost zero; however, by adding triethylamine at a concentration of 1.0 mol·L^{-1}, the H_2 production was greatly improved. This is mainly because in the solution containing only water molecules, although the RGO could transfer electrons well, the holes (h^+) on the surface were not well transferred or consumed, thus making the holes and electrons easy to recombine, leading to the almost zero H_2 production; however, after adding triethylamine in the solution, the holes (h^+) were consumed through the oxidation reaction with the triethylamine adsorbed on the surface of RGO/$ZnIn_2S_4$, thus reducing the hole and electron recombination, making the H_2 production greatly improved. At the same time, triethylamine was eventually decomposed into carbon dioxide, ammonia, and water.[22] In addition, when triethylamine was used as the sacrificial agent, the H_2 production reached 1597 μmol·g^{-1}·h^{-1}, which was 2.6 times as high as that obtained using the aqueous solution mixture of Na_2S and Na_2SO_3 as the sacrificial agent.

It can also be seen from Figure 1 that when the organic amine concentration was 1.0 mol·L^{-1}, the catalyst concentration was 1.0 g·L^{-1}, and the solution pH was 13, the order of H_2 production rate in the six organic amines was triethylamine ($N(CH_2CH_3)_3$) > triethanolamine ($(HOCH_2CH_2)_3N$) > trimethylamine ($N(CH_3)_3$) > ethanolamine ($HO(CH_2)_2NH_2$) > aniline (C_6H_5–N_2) > urea ($CO(NH_2)_2$). Among them, the activity order of $N(CH_2CH_3)_3$ > $(HOCH_2CH_2)_3N$ > $HO(CH_2)_2NH_2$ was consistent with the results reported by Li et al.[23] According to Li, because of the strong electronegativity of the N atom, the electron density cloud of the adjacent $-CH_2-$ is reduced, making it vulnerable to be attacked by hydroxyl radical; in addition, the N atom and the photocatalyst can form a stable coordination bond, so that $N(CH_2CH_3)_3$ can be easily adsorbed on the surface of the photocatalyst and can be easily degraded by photocatalysis.[23] The combined effect makes the h^+ easier to consume, the recombination rate of the photogenerated electron–hole pairs much lower, and the H_2 production greatly improved. As for $(HOCH_2CH_2)_3N$ in the present study because the electronegativity of the O atom (3.44) in it was stronger than that of the N atom (3.04), the electrons at the N atom and the $-CH_2-$ were shifted toward the O atom, which increased the electron density cloud of $-CH_2-$ near the O atom. As a result, the ability of hydroxyl radical to attack $-CH_2-$ weakened, which made the photocatalytic H_2 production in $(HOCH_2CH_2)_3N$ solution lower than that in $N(CH_2CH_3)_3$. For $N(CH_3)_3$, the stability of its $-CH_3$ was stronger than that of its $-CH_2-$, so its ability of being oxidized by hydroxyl radicals was weakened, which caused the photocatalytic H_2 production lower than that in $(HOCH_2CH_2)_3N$ solution. As for $CO(NH_2)_2$ and C_6H_5–N_2, the former contained the p–π conjugation formed by the carbonyl group and two $-NH_2$, whereas the latter contained the p–π conjugation formed by the benzene ring and N atoms; the conjugated structure made the internal energy in the molecules reduced, so that the molecules tended to be stable. Therefore, they were difficult to be oxidized by hydroxyl radicals, so that their recombination of the photon hole–electron pair greatly increased, resulting in the H_2 production being almost zero.

2.2. Effects of Reaction Conditions on H_2 Production When Using Triethylamine as Sacrificial Agent. *2.2.1. Effects of the pH Values of the Solutions on H_2 Production.* Figure 2 shows the photocatalytic H_2 production efficiency with $N(CH_2CH_3)_3$ as the sacrificial agent at the solutions with

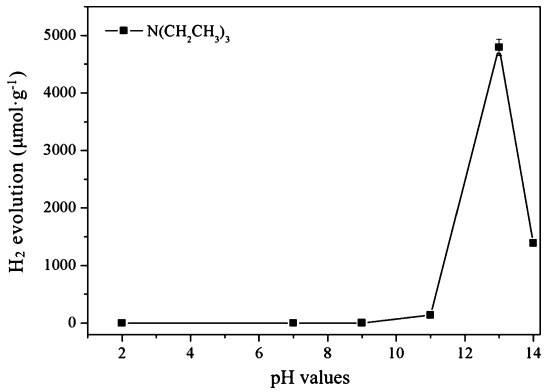

Figure 2. Photocatalytic H_2 production with triethylamine as sacrificial agent at different pH values.

DOI: 10.1021/acsomega.9b01034
ACS Omega 2019, 4, 11135–11140

different pH values (2, 7, 9, 11, 13, 14). It can be seen that the H_2 production was zero under either neutral or acidic conditions; when the pH was 9, H_2 production increased; when the pH was 13, the H_2 production efficiency was the highest; as the pH continued to increase, H_2 production dropped sharply. These results are mainly because, at different pH values, $N(CH_2CH_3)_3$ was adsorbed on the catalyst surface in different forms. When the pH of the solution was acidic or neutral (where the solution pH was adjusted with HCl), $N(CH_2CH_3)_3$ was more likely to combine with hydrochloric acid to form triethylamine hydrochloride, which reduced the amount of triethylamine adsorbed on the catalyst surface, thus increasing the recombination rate of the photogenerated electron−hole pairs, hence reducing H_2 production to a very low level or even zero. However, when the pH of the $N(CH_2CH_3)_3$ solution was 13, most of the $N(CH_2CH_3)_3$ existed in molecular form, which could be well adsorbed on the surface of the catalyst, so as to accelerate the separation of photogenerated electron−hole pairs, thus greatly improving H_2 production. When the pH of $N(CH_2CH_3)_3$ was higher than 13, the reduction potential of H^+/H_2 became very low and was not conducive to the generation of H_2, resulting in a sharp decrease in H_2 production.

2.2.2. Effects of the Concentration of RGO/$ZnIn_2S_4$ on H_2 Production. Figure 3 shows the photocatalytic H_2 production

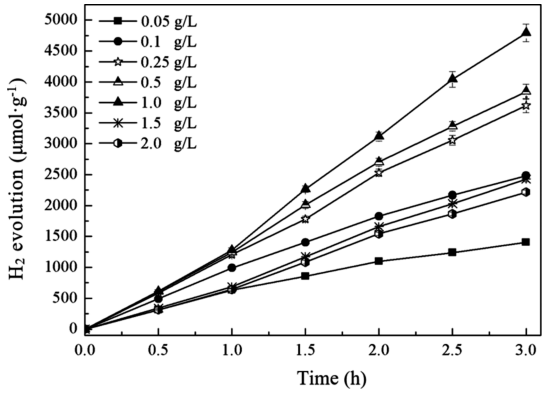

Figure 3. Photocatalytic H_2 production with triethylamine as the sacrificial agent at different RGO/$ZnIn_2S_4$ dosages.

efficiency with $N(CH_2CH_3)_3$ as the sacrificial agent at different RGO/$ZnIn_2S_4$ dosages (0.05−2.0 g·L^{-1}). It can be seen that, with the increase of catalyst concentration, the corresponding H_2 production showed a trend of increasing first and then decreasing; in particular, when the concentration was 1.0 g·L^{-1}, H_2 production was the highest. This result is mainly because when the RGO/$ZnIn_2S_4$ concentration (0.05 g·L^{-1}) was low, the reaction active sites of the catalyst were less, so it could not fully and effectively use the light energy, leading to low H_2 production; when the RGO/$ZnIn_2S_4$ concentration gradually increased to 1.0 g·L^{-1}, the reaction active sites of the catalyst increased as well, the catalyst could fully and effectively use the light energy to contact and react with $N(CH_2CH_3)_3$, which increased the H_2 production; when the concentration of RGO/$ZnIn_2S_4$ continued to increase, the over high concentration caused shading, which reduced the efficiency of the catalyst to accept photons, leading to a decrease in the H_2 production.

2.2.3. Effects of Triethylamine Concentrations on H_2 Production. Figure 4 shows the photocatalytic H_2 production efficiency with $N(CH_2CH_3)_3$ of different concentrations

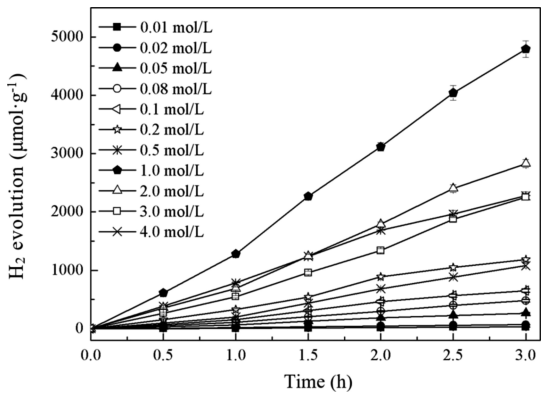

Figure 4. Photocatalytic H_2 production with triethylamine of different concentrations as sacrificial agents.

(0.01−4.0 mol·L^{-1}) as sacrificial agents. As can be seen from Figure 4, with the increase of $N(CH_2CH_3)_3$ concentration, the corresponding H_2 production showed a tendency to increase first and then decrease, with the highest appearing at the concentration of 1.0 mol·L^{-1}. This result is mainly because when the $N(CH_2CH_3)_3$ concentration was lower than 1.0 mol·L^{-1}, 1.0 g·L^{-1} of the catalyst was not fully used; as the concentration increased from 0.1 to 1.0 mol·L^{-1}, the utilization of the catalyst in the unit time was improved, so that the corresponding H_2 production gradually increased; when the $N(CH_2CH_3)_3$ concentration was higher than 1.0 mol·L^{-1}, the surface active sites of RGO/$ZnIn_2S_4$ were limited, so H_2 production was gradually reduced.

2.3. Photocatalytic Test under Sunlight. Figure 5a shows the photocatalytic H_2 production with sunlight as a light source, the corresponding light intensities of which are shown in Figure 5b. The test conditions were as follows: 1.0 mol·L^{-1} of $N(CH_2CH_3)_3$, 1.0 g·L^{-1} of catalyst, and the solution pH was 13. The solar-light-driven experiments were carried out for 3 days, between 9:25 and 17:25 each day on August 16 to August 18, 2015, at the E building roof of the Harbin Institute of Technology (Shenzhen), which is located in Shenzhen, China (N 22.59°, E 113.97°). As can be seen from Figure 5a, for the first 5 h of the reaction, all H_2 production by RGO/$ZnIn_2S_4$ in the 3 days showed a tendency to increase gradually; at 14:25, all H_2 production rates of the 3 days reached the maximum, that is 265, 121, and 423 μmol·g^{-1}·h^{-1}, respectively. When the reaction time exceeded 5 h, H_2 production basically remained unchanged in a range of error. This is mainly because after 14:25, the intensity of the sunlight weakened, so that the photocatalytic reaction tended to stop. In addition, as can be seen from Figure 5a, H_2 production of the 3 days differed significantly, with the production order being day 3 > day 1 > day 2. This is because within the first 5 h of the photocatalytic hydrogen production process, the sunlight intensity on day 3 was higher than that on either day 1 or day 2 and remained on a high level, so the H_2 production on day 3 was the highest; and the sunlight intensity on day 1 increased gradually and was correspondingly higher than that on day 2, so that the H_2 production rate on day 1 was higher than on day 2. It can be seen that the light intensity had a significant effect on H_2 production by the catalyst. It is worth noting that, although this experiment was carried out in the winter, in the case of strong sunlight, the H_2 production activity of the catalyst could be up to 26% of laboratory (350 W Xe lamp) results.

DOI: 10.1021/acsomega.9b01034
ACS Omega 2019, 4, 11135−11140

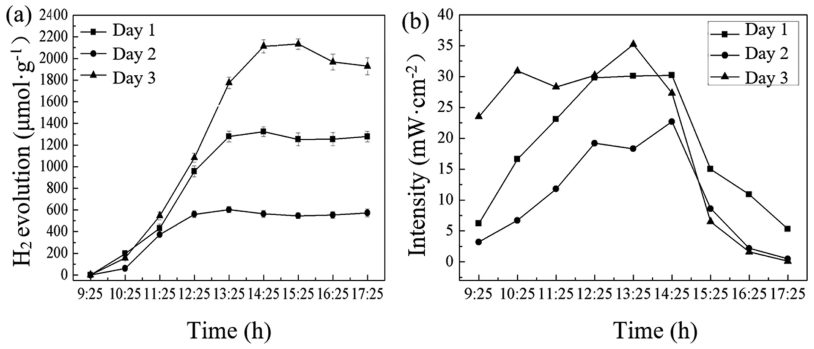

Figure 5. Photocatalytic H_2 production with sunlight as a light source and the corresponding light intensities. (a) H_2 production; (b) light intensity.

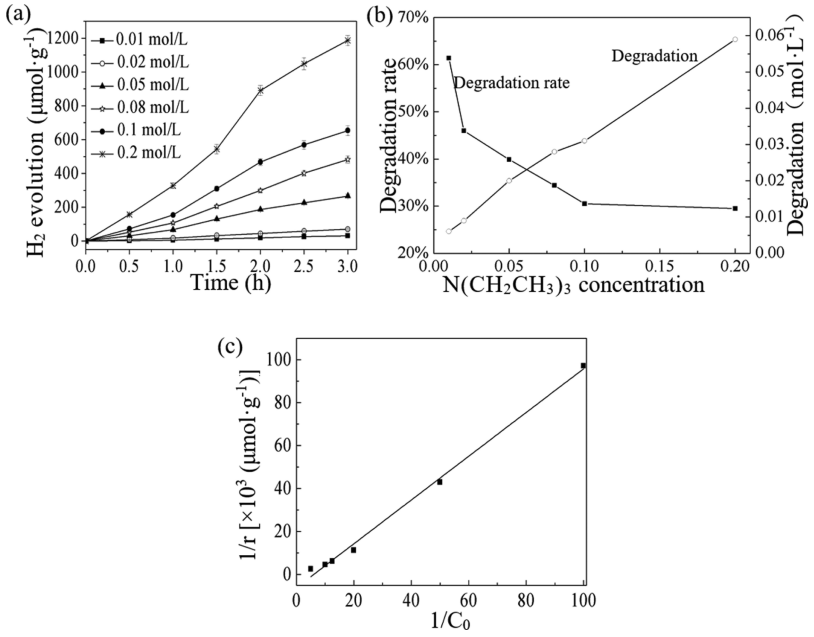

Figure 6. Simultaneous H_2 production and organic degradation in low trimethylamine-concentration solutions and the corresponding kinetics analysis. (a) H_2 production in low trimethylamine-concentration solution; (b) degradation of trimethylamine in different trimethylamine-concentration solutions; (c) kinetic analysis.

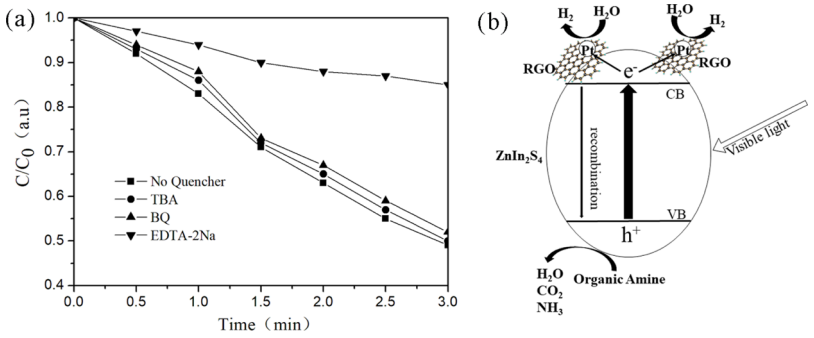

Figure 7. (a) Trapping experiments of the active species during the photocatalytic degradation of triethylamine over RGO/$ZnIn_2S_4$ sample under visible light irradiation. (b) Proposed photocatalytic mechanism of RGO/$ZnIn_2S_4$.

2.4. Kinetic Study of H_2 Production Using Low-Concentration Triethylamine as Sacrificial Agent. Taking into account that the actual concentration of $N(CH_2CH_3)_3$ in wastewater is not high, this study selected low-concentration (0.01−0.2 mol·L^{-1}) $N(CH_2CH_3)_3$ wastewater as the reaction solution to look at its degradation in the process of photocatalytic H_2 production. Figure 6a,b show the simultaneous H_2 production and the $N(CH_2CH_3)_3$ degradation when using the low-concentration $N(CH_2CH_3)_3$ as the sacrificial agent. As shown in Figure 6a, when the $N(CH_2CH_3)_3$ concentration was low, with the increase of $N(CH_2CH_3)_3$ concentration, the corresponding H_2 production showed a gradually rising trend. As can be seen from Figure 6b, with the increase of $N(CH_2CH_3)_3$ concentration, although the degradation rate of $N(CH_2CH_3)_3$ gradually decreased, the total degradation amount gradually increased instead. It can be

DOI: 10.1021/acsomega.9b01034
ACS Omega 2019, 4, 11135−11140

seen that when $N(CH_2CH_3)_3$ in the wastewater was used as the sacrificial agent, hydrogen production and degradation of $N(CH_2CH_3)_3$ can occur simultaneously.

Figure 6c shows the kinetic analysis of the effect of $N(CH_2CH_3)_3$ concentration on H_2 production. As can be seen from Figure 6c, after linear transformation, H_2 production was linear with the change of $C_6H_{15}N$ concentration. The line met the characteristics of the Langmuir equation

$$kKC/(KC + 1) = r$$

where r, C, k, K are the hydrogen production rate, triethylamine concentration, surface reaction rate constant, and apparent adsorption equilibrium constant, respectively. By calculation, the apparent reaction constant k is 1.64×10^{-4} mol·h^{-1}, the apparent adsorption equilibrium constant K is 5.97×10^{-3} L·mol^{-1}, and R^2 is 0.995.

2.5. Photocatalytic Oxidation Mechanism of Triethylamine. The detection of main oxides in a photocatalytic process is of great significance to reveal the photocatalytic mechanism. In the presence of *tert*-butyl alcohol (TBA, hydroxyl radical scavenger), 1,4-benzoquinone (BQ, superoxide radical scavenger), or disodium acetate (EDTA−2Na, hole scavenger), the main oxidation products in the photocatalytic degradation of triethylamine were detected by free radical and hole trapping experiments. As shown in Figure 7a, under visible light irradiation, the photodegradation rate of triethylamine decreased slightly with the addition of TBA and BQ, indicating that the hydroxyl radical and superoxide radical were not the main active substances for the degradation of triethylamine in these photocatalytic systems. However, the photodegradation rate of triethylamine decreased significantly with the addition of EDTA−2Na. The above results show that the holes play a major role in the degradation of triethylamine in RGO/$ZnIn_2S_4$ photocatalytic systems under visible light irradiation.

Based on the above experimental results, the degradation mechanism of triethylamine in RGO/$ZnIn_2S_4$ photocatalysis was proposed and is shown in Figure 7b. When $ZnIn_2S_4$ is irradiated with visible light, electrons will be excited to the conduction bands (CB), whereas holes will remain in the valence bands (VB). The electrons in the CB rapidly transported to the surface of Pt particles through RGO, and reacted with H_2O to produce H_2. Holes in the VB reacted with triethylamine and degraded them.

3. CONCLUSIONS

The presence of organic amine can promote hydrogen production from decomposition of water. The order of H_2 generation activity of RGO/$ZnIn_2S_4$ in six organic amine solutions was $N(CH_2CH_3)_3$ > $N(HOCH_2CH_2)_3$ > $N(CH_3)_3$ > $HO(CH_2)_2NH_2$ > $C_6H_5{-}N_2$> $CO(NH_2)_2$, and the highest H_2 production was in $N(CH_2CH_3)_3$ solution, being 1597 μmol·g^{-1}·h^{-1}, 2.6 times as high as that by using the aqueous solution mixture of Na_2S and Na_2SO_3 as sacrificial agent. In addition, when the pH was 13, the catalyst concentration was 1.0 g·L^{-1}, and the $N(CH_2CH_3)_3$ concentration was 1.0 mol·L^{-1}, the photocatalytic activity was the highest. When $N(CH_2CH_3)_3$ in wastewater is used as sacrificial agent, hydrogen production and degradation of $N(CH_2CH_3)_3$ can occur simultaneously. The holes play a major role in the degradation of $N(CH_2CH_3)_3$ in RGO/$ZnIn_2S_4$ photocatalytic systems under visible light irradiation; the relationship between the concentration of $N(CH_2CH_3)_3$ and H_2 production was in accordance with the Langmuir equation.

4. EXPERIMENTAL SECTION

4.1. Materials. All chemicals were of analytical grade and used as received without further purification. $In(NO_3)_3{\cdot}4H_2O$, $ZnSO_4{\cdot}7H_2O$, H_2O_2 (30%), thioacetamide (TAA), potassium permanganate (K_2MnO_4), H_2SO_4 (purity ≥98%), $NaNO_3$, absolute ethanol, glycerol, and organic amines(including triethylamine, triethanolamine, trimethylamine, ethanolamine, aniline, and urea) were purchased from Sinopharm Chemical Reagent Co., Ltd., China. Na_2S and Na_2SO_3 (purity ≥99.99%) were purchased from Sinopharm Chemical Reagent Co., Ltd., China. $H_2PtCl_6{\cdot}6H_2O$ (purity ≥99.99%) was purchased from Shanghai July Chemical Co., Ltd., China. Graphite was purchased from Aladdin Reagent (Shanghai) Co., Ltd., China.

4.2. Preparation of RGO/$ZnIn_2S_4$. The RGO/$ZnIn_2S_4$ sample was prepared by an alcohothermal method. The preparation steps are consistent with the optimal procedure for the preparation of RGO/$ZnIn_2S_4$ in our previous work[25] and are only briefly described herein.

For the synthesis of GO, graphite powder (5 g) and $KMnO_4$ (20 g) were added into a flask (500 mL); then the mixture was vigorously stirred at 10 °C for 30 min and at 35 °C for 5 h, until a thick paste formed. Then, the mixture was diluted by deionized water (300 mL), treated with ultrasonic for 3 h, and diluted with distilled water (200 mL). The residual $KMnO_4$ was destroyed through reduction by H_2O_2 (20 mL, 30%). Subsequently, the mixture was sufficiently washed with dilute HCl solution (5%) and deionized water. After drying in an air oven at 65 °C overnight, GO powder was obtained. The GO powder was then dispersed in absolute ethanol and washed 3 times with absolute ethanol, then a GO suspension was obtained. The as-prepared GO suspension was used directly in the next synthesis procedure.

For the synthesis of $ZnIn_2S_4$, $ZnSO_4{\cdot}7H_2O$ (0.735 g), $In(NO_3)_3{\cdot}4H_2O$ (1.903 g), and TAA were dissolved in the solution mixed by absolute ethanol (40 mL) and glycerol (10 mL). The mixed solution (solution-1) was stirred for 30 min and then hydrothermally treated at 180 °C for 12 h, then cooled to room temperature naturally. A yellow precipitate was obtained, then filtered and washed with absolute ethanol and deionized water three times. After drying in vacuum at 80 °C, $ZnIn_2S_4$ was obtained.

For the synthesis of 0.1 wt % RGO/$ZnIn_2S_4$, a desired amount of GO was dropped into the solution-1 before heating.

4.3. Photocatalytic Reaction. Photocatalytic tests were carried out in an 868 mL gastight stainless steel reactor. The specific reactor characteristics were introduced in detail in our previous work.[20,25] The light source was a 350 W Xe lamp (Shenzhen Stone-lighting Opto Device Co., Ltd., China), and a cut-off filter was used to remove the UV part of the light (λ > 420 nm). The light intensity was measured using a spectroradiometer (FZ-A, Photoelectric Instrument Factory of Beijing Normal University).

In all experiments, 200 mL deionized water containing a desired amount of catalyst (0.05, 0.1, 0.25, 0.5, 1.0, 1.5, or 2.0 g·L^{-1}) and organic amine(0.01, 0.02, 0.05, 0.08, 0.1, 0.2, 0.5, 1.0, 2.0, 3.0, or 4.0 mol·L^{-1}) was added into the reactor. Before light irradiation, argon gas was bubbled through the reaction mixture for 30 min to remove air from the reaction solution. Pt as a cocatalyst for the promotion of hydrogen evolution was photodeposited in situ on the photocatalyst from the precursor

DOI: 10.1021/acsomega.9b01034
ACS Omega 2019, 4, 11135−11140

of $H_2PtCl_6{\cdot}6H_2O$, when there was special instruction. Hydrogen evolution was analyzed with a gas chromatograph (Shanghai Precision & Scientific Instrument Co., Ltd., GC-112A). Samples were taken at intervals of 60 min at 500 μL. Degradation of organic amines was analyzed in a high performance liquid chromatograph (LC2000, Shanghai Techcomp Instrument Ltd, China) using a Symmetry C18 column and a mobile phase consisting of 70% methanol (chromatographic pure) and 30% water. Before light irradiation, the suspension was stirred for 60 min in the dark to attain adsorption−desorption equilibrium of the organic amines on the surface of the photocatalyst. During the reaction, 2 mL suspension was withdrawn from the reaction vessel every 60 min. The photocatalyst was removed from the suspension by centrifugation.

AUTHOR INFORMATION

Corresponding Author

*E-mail: rszhu@hit.edu.cn.

ORCID

Rongshu Zhu: 0000-0001-5589-9031

Notes

The authors declare no competing financial interest.

ACKNOWLEDGMENTS

All authors gratefully acknowledge support from the Special Fund for the Development of Strategic and New Industry in Shenzhen (no. JCYJ20150731104949789) and the Fund for Knowledge Innovation in Shenzhen (no. JCYJ20180507183621817).

REFERENCES

(1) Zhou, P.; Yu, J.; Jaroniec, M. All-solid-state Z-scheme photocatalytic systems. *Adv. Mater.* **2014**, *26*, 4920−4935.

(2) Ma, X.; Jiang, Q.; Guo, W.; Zheng, M.; Xu, W.; Ma, F.; Hou, B. Fabrication of g-C_3N_4/Au/CdZnS Z-scheme photocatalyst to enhance photocatalysis performance. *RSC Adv.* **2016**, *6*, 28263−28269.

(3) Hao, L.; Kang, L.; Huang, H.; Ye, L.; Han, K.; Yang, S.; Yu, H.; Batmunkh, M.; Zhang, Y.; Ma, T. Surface-Halogenation-Induced Atomic-Site Activation and Local Charge Separation for Superb CO_2 Photoreduction. *Adv. Mater.* **2019**, 1900546.

(4) Yu, J.; Ran, J. Facile preparation and enhanced photocatalytic H_2-production activity of $Cu(OH)_2$ cluster modified TiO_2. *Energy Environ. Sci.* **2011**, *4*, 1364.

(5) Xing, M.; Qiu, B.; Du, M.; Zhu, Q.; Wang, L.; Zhang, J. Spatially Separated CdS Shells Exposed with Reduction Surfaces for Enhancing Photocatalytic Hydrogen Evolution. *Adv. Funct. Mater.* **2017**, *27*, 1702624.

(6) Zheng, D.; Pang, C.; Wang, X. The function-led design of Z-scheme photocatalytic systems based on hollow carbon nitride semiconductors. *Chem. Commun.* **2015**, *51*, 17467−17470.

(7) Zhang, L. J.; Li, S.; Liu, B. K.; Wang, D. J.; Xie, T. F. Highly Efficient CdS/WO_3 Photocatalysts: Z-Scheme Photocatalytic Mechanism for Their Enhanced Photocatalytic H_2 Evolution under Visible Light. *ACS Catal.* **2014**, *4*, 3724−3729.

(8) Yu, J.; Wang, S.; Low, J.; Xiao, W. Enhanced photocatalytic performance of direct Z-scheme g-C_3N_4-TiO_2 photocatalysts for the decomposition of formaldehyde in air. *Phys. Chem. Chem. Phys.* **2013**, *15*, 16883−16890.

(9) Li, S.; Zhao, Q.; Wang, D.; Xie, T. Work function engineering derived all-solid-state Z-scheme semiconductor-metal-semiconductor system towards high-efficiency photocatalytic H_2 evolution. *RSC Adv.* **2016**, *6*, 66783−66787.

(10) Nagaraju, G.; Manjunath, K.; Sarkar, S.; Gunter, E.; Teixeira, S. R.; Dupont, J. TiO_2−RGO hybrid nanomaterials for enhanced water splitting reaction. *Int. J. Hydrogen Energy* **2015**, *40*, 12209−12216.

(11) Saadetnejad, D.; Yıldırım, R. Photocatalytic hydrogen production by water splitting over Au/Al-$SrTiO_3$. *Int. J. Hydrogen Energy* **2018**, *43*, 1116−1122.

(12) Chen, P.; Dong, F.; Ran, M.; Li, J. Synergistic photo-thermal catalytic NO purification of MnO x /g-C_3N_4 : Enhanced performance and reaction mechanism. *Chin. J. Catal.* **2018**, *39*, 619−629.

(13) Li, J.; Zhang, Z.; Cui, W.; Wang, H.; Cen, W.; Johnson, G.; Jiang, G.; Zhang, S.; Dong, F. The Spatially Oriented Charge Flow and Photocatalysis Mechanism on Internal van der Waals Heterostructures Enhanced g-C_3N_4. *ACS Catal.* **2018**, *8*, 8376−8385.

(14) Cui, W.; Chen, L.; Li, J.; Zhou, Y.; Sun, Y.; Jiang, G.; Lee, S. C.; Dong, F. Ba-vacancy induces semiconductor-like photocatalysis on insulator $BaSO_4$. *Appl. Catal., B* **2019**, *253*, 293−299.

(15) Chen, F.; Huang, H.; Guo, L.; Zhang, Y.; Ma, T. The Role of Polarization in Photocatalysis. *Angew Chem Int Ed Engl* **2019**, *58*, 2−15.

(16) Salvador, P.; Garcia Gonzalez, M. L. G. Catalytic Role of Lattice Defects in the Photoasslsted Oxidation of Water at (001)n-TiO_2 Rutile. *J. Phys. Chem.* **1992**, *96*, 10349−10353.

(17) Munoz, P.; Malekshoar, G.; Ray, M. B.; Zhu, J.; Ray, A. K. Sacrificial Hydrogen Generation from Formaldehyde with Pt/TiO_2 Photocatalyst in Solar Radiation. *Ind. Eng. Chem. Res.* **2013**, *52*, 5023−5029.

(18) Speltini, A.; Sturini, M.; Maraschi, F.; Dondi, D.; Fisogni, G.; Annovazzi, E.; Profumo, A.; Buttafava, A. Evaluation of UV-A and solar light photocatalytic hydrogen gas evolution from olive mill wastewater. *Int. J. Hydrogen Energy* **2015**, *40*, 4303−4310.

(19) Gao, H.; Zhang, J.; Wang, R.; Wang, M. Highly efficient hydrogen production and formaldehyde degradation by Cu_2O microcrystals. *Appl. Catal., B* **2015**, *172*−*173*, 1−6.

(20) Zhu, R.; Tian, F.; Yang, R.; He, J.; Zhong, J.; Chen, B. Z scheme system $ZnIn_2S_4$/RGO/$BiVO_4$ for hydrogen generation from water splitting and simultaneous degradation of organic pollutants under visible light. *Renewable Energy* **2019**, *139*, 22−27.

(21) Wu, Y.; Lv, G.; Li, B. Hydrogen Production by Pt/TiO_2 Anaerobic Photocatalytic Reforming Degradation of Aqueous Monoethanolamine. *Acta Phys.—Chim. Sin.* **2004**, *20*, 755−758.

(22) Yin, Z.; Li, Y.; Peng, S.; Lu, G.; Li, S. Photocatalytic Hydrogen Generation in the Presence of Ethanolamines over Pt/TiO_2. *J. Mol. Catal.* **2007**, *21*, 155−161.

(23) Li, Y.; Zhang, K.; Peng, S.; Lu, G.; Li, S. Photocatalytic hydrogen generation in the presence of ethanolamines over Pt/$ZnIn_2S_4$ under visible light irradiation. *J. Mol. Catal. A: Chem.* **2012**, *363*−*364*, 354−361.

(24) Peng, S.; Ding, M.; Yi, T.; Li, Y. Photocatalytic Hydrogen Evolution in the Presence of Pollutant Methylamines over Pt/$ZnIn_2S_4$ under Visible Light Irradiation. *J. Mol. Catal.* **2014**, *5*, 466−473.

(25) Tian, F.; Zhu, R.; Zhong, J.; Wang, P.; Ouyang, F.; Cao, G. An efficient preparation method of RGO/$ZnIn_2S_4$ for photocatalytic hydrogen generation under visible light. *Int. J. Hydrogen Energy* **2016**, *41*, 20156−20171.

DOI: 10.1021/acsomega.9b01034
ACS Omega 2019, 4, 11135−11140